Functional Nanocrystals

DOI: 10.1002/ange.201005775

Surfactant-Free Platinum-on-Gold Nanodendrites with Enhanced Catalytic Performance for Oxygen Reduction**

Kyung Min Yeo, Suhee Choi, Rahman Md Anisur, Jongwon Kim, and In Su Lee**

Platinum and its alloys play important roles in many industrial applications, such as CO/NO_x oxidation in catalytic converters, synthesis of nitric acid, oil cracking, and fuel cells.[1] In particular, platinum has been the most effective catalyst in proton-exchange membrane fuel cells (PEMFCs) owing to its outstanding electrocatalytic characteristics, which facilitate both hydrogen oxidation and oxygen reduction. Although carbon-supported platinum nanoparticles are currently used as cathode catalysts in fuel-cell technology, the commercialization of this technology for automotive applications still requires more economical and effective catalytic materials that can operate with a much smaller amount of expensive platinum.[2] Over the last decade, pioneering researchers reported that the electrocatalytic performance of platinum-based materials can be improved by controlling the morphology of platinum nanocrystals or alloying platinum with other transition metals.[3–5] In particular, the recently developed platinum nanocrystals with dendritic structures displaying a large number of edges and corner atoms exhibit dramatically enhanced catalytic activity in the oxygen reduction reaction (ORR), the slow kinetics of which is a major problem limiting the efficiency of PEMFCs.[6] Although there has been considerable progress in the preparation of platinum nanodendrites through metal seed or block copolymer mediated processes, the lack of a facile synthetic route has limited the practical applications of nanodendrites.[7–10] In particular, there is strong demand for a new synthetic method for the mass production of nanodendrites. In this context, the study described herein examines the possibility of large-scale synthesis of platinum nanodendrites in a controllable manner using the recently developed hollow nanoreactor, consisting of a porous silica nanoshell and an entrapped Au nanocrystal, which can confine the growth of metal species inside the silica cavity.[11] The hollow silica nanoreactors provide a consistent and well-isolated environment for the growth of nanocrystals, which enables the morphology-controlled synthesis of Pt nanodendrites even from a highly concentrated reaction suspension. Moreover, the porous silica shell can be removed readily under basic conditions, leaving a Pt nanodendrite in a surfactant-free form. The surfactant-free Pt dendrites were ready for catalytic applications without additional surfactant-removing processes under harsh conditions, which frequently cause the deformation of the nanocrystals and the decline of catalytic activities. In addition, the surfactant-free nature of the nanocrystals could make it possible to lend the surface various properties and functions through simply coordination of functional ligand molecules.

Herein we report the novel synthesis of Pt nanodendrites by Au-seed-mediated growth inside hollow silica nanospheres. The proposed synthetic protocol based on isolated nanoreactors is quite remarkable in terms of the product yield per unit reaction volume compared to traditional capping-agent-based synthesis, which produces only a few milligrams of Pt nanodendrites per milliliter of reaction suspension. The nanoreactor-based synthetic route enabled the synthesis of as much as 1.5 g of uniform Pt nanodendrites from a single reaction in 40 mL aqueous suspension. The prepared ligand-free Pt nanodendrites exhibited greater ORR activity than commercial Pt black catalysts. We also report the extendable utility of the current method to prepare Pt nanodendrite colloid with tunable dispersity and hybrid nanocrystals of various metals.

Scheme 1 summarizes the general synthetic routes for various Pt-based nanoparticles based on seed-mediated growth inside porous hollow silica nanospheres. The hollow nanoreactor (Au@*h*-SiO_2), which consists of a porous silica nanoshell with inner and outer diameters of (14 ± 2) and (28 ± 2) nm, respectively, and a (4.0 ± 0.6) nm Au nanocrystal captured inside the cavity, was prepared by selective etching of Fe_3O_4 from a silica nanosphere encapsulating a Fe_3O_4/Au hybrid nanocrystal.[11] When an aliquot of Na_2PtCl_4 was added to an aqueous suspension containing Au@*h*-SiO_2 nanospheres

[*] K. M. Yeo, R. M. Anisur, Prof. I. S. Lee
Department of Applied Chemistry, Kyung Hee University
Gyeonggi-do 446-701 (Korea)
E-mail: insulee97@khu.ac.kr
S. Choi, Prof. J. Kim
Department of Chemistry, Chungbuk National University
Chungbuk 361-763 (Korea)
E-mail: jongwonkim@chungbuk.ac.kr

[**] This research was supported by the Basic Science Research Program through the National Research Foundation of Korea (NRF) funded by the Ministry of Education, Science, and Technology (2010-0003950) (I.S.L.) and (2010-0004126) (J.K.).

Supporting information for this article is available on the WWW under http://dx.doi.org/10.1002/anie.201005775.

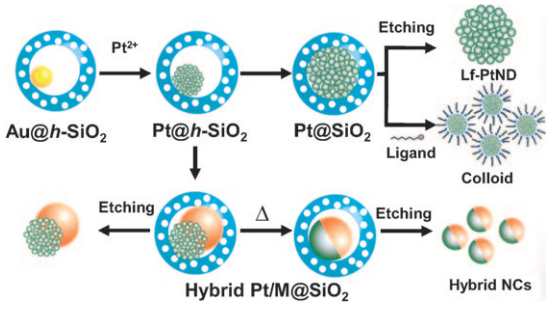

Scheme 1. The synthesis of platinum-based nanodendrites and hybrid nanocrystals.

(0.4 mg mL^{-1}) and L-ascorbic acid (2.88 mg mL^{-1}) with constant stirring, the reddish brown color gradually darkened, and an opaque black suspension was generated within 1 h (Figure 1 a). Transmission electron microscopy (TEM) and

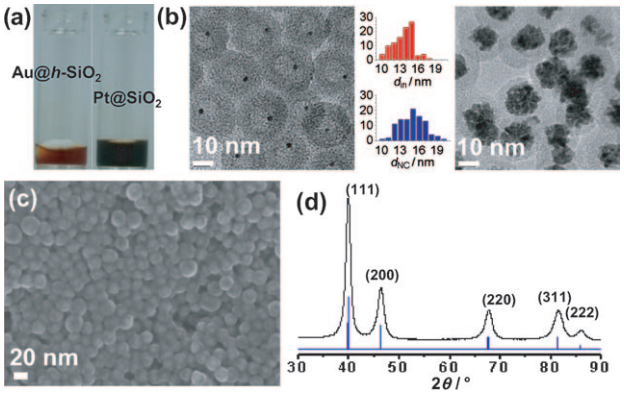

Figure 1. a) Photographs of the reaction suspensions before (left) and after (right) the Pt growth reaction with Au@*h*-SiO$_2$. b) TEM images of Au@*h*-SiO$_2$ (left) and Pt@SiO$_2$ (right) nanospheres, and histograms showing the distribution of the cavity size d_{in} of Au@*h*-SiO$_2$ (top) and the diameter d_{NC} of the Pt-on-Au nanodendrite of Pt@SiO$_2$ (bottom). c) SEM image of Pt@SiO$_2$. d) XRD pattern of Pt@SiO$_2$. The blue trace shows the position of the reflections corresponding to fcc Pt phase (JCPDS Card No. 87-0646).

scanning electron microscopy (SEM) of the isolated black powder confirmed the confined growth of Pt species exclusively inside the hollow cavity to create Pt@SiO$_2$ nanospheres in which a Pt-on-Au nanocrystal with 3D flowerlike morphology was well-coated with a porous silica shell (Figure 1 b,c). X-ray diffraction (XRD) revealed the formation of Pt crystals with face-centered-cubic (fcc) crystalline phase (Figure 1 d). The average size of Pt grains of Pt@SiO$_2$ was estimated to be 4 nm using the Scherrer equation based on the peak width in the XRD pattern. Larger Pt nanocrystals were formed when the initial concentration of Na_2PtCl_4 was increased from 0.02 to 2.0 mg mL^{-1}, but their maximum size was limited to (15 ± 2) nm even at higher concentrations of Na_2PtCl_4. This finding indicates the preferential nucleation of Pt exclusively at the Au surface inside the cavity, with subsequent gradual growth that is restricted by the cavity size (see Figure S1 in the Supporting Information).[12] Control reactions with hollow silica nanospheres in the absence of an Au seed (*h*-SiO$_2$) or with Au nanoparticles stabilized by citrates resulted in the growth of large Pt particles on the outer surface of the silica spheres and the formation of large aggregates of Pt nanoparticles, respectively (see Figure S2 in the Supporting Information).

High-resolution TEM (HRTEM) of Pt@SiO$_2$ showed that the grown nanocrystal has a three-dimensional dendritic structure with interconnected Pt arms (Figure 2 d). Individual Pt arms have an average size of (3.0 ± 0.4) nm and show a single crystalline structure enclosed mainly by (111) facets and a small fraction of (311) facets, which is consistent with the selective area electron diffraction (SAED) pattern

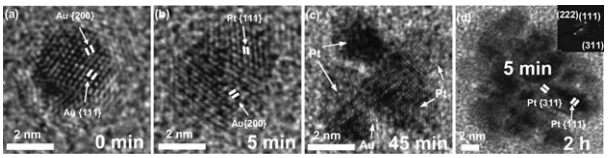

Figure 2. HRTEM images of the samples obtained from the suspension of Au@*h*-SiO$_2$, Na_2PtCl_4, and L-ascorbic acid a) at the beginning of the reaction and after reaction for b) 5 min, c) 45 min, and d) 2 h. The inset shows the SAED pattern of the Pt-on-Au nanodendrite grown inside Pt@SiO$_2$.

obtained during TEM analysis. The weight percentage of Pt in the (15 ± 2) nm Pt-on-Au nanodendrites was 99 % according to inductively coupled plasma atomic-emission spectroscopy (ICP-AES). HRTEM images obtained from the initial period of the reaction showed that Pt nucleated at single sites on the (111) surface of the single-crystalline Au seed and grew epitaxially along the (111) direction (Figure 2 a,b). The single-site nucleation of Pt can be understood by blockage of the remaining possible nucleation sites on the Au seed by the silica surface of the cavity. Further growth occurred preferentially on the Pt nuclei rather than the Au surface, most likely by an autocatalyzing process at the preformed Pt surface.[6a,7d,13] As the reaction proceeded, additional Pt buds appeared from multiple sites on the pregrown Pt arm and branched out to other arms, thus developing into dendritic tendrils (Figure 2 c).

The ligand-free Pt-on-Au nanodendrites (Lf-PtND) could be readily isolated from the Pt@SiO$_2$ without significant changes in their morphology by dissolving the silica shell in a dilute basic solution at room temperature. TEM and HRTEM images of the powder collected after immersing the Pt@SiO$_2$ in a 2.0 M NaOH solution for 30 min showed that the Lf-PtND has a clean surface without capping surfactants (Figure 3 a).

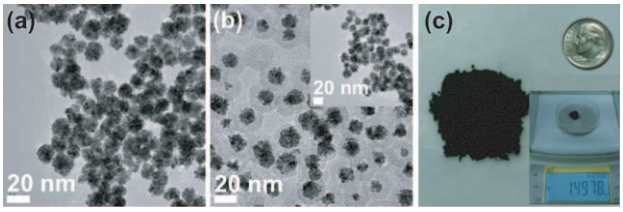

Figure 3. a) TEM image of Lf-PtND. b) TEM images of Pt@SiO$_2$ and Lf-PtND (inset) obtained from a gram-scale synthesis reaction. c) Photograph of 1.5 g of Lf-PtND powder obtained from a single reaction.

XRD analysis of Lf-PtND did not show any significant change in crystalline phase or grain size during the etching process (see Figure S3 in the Supporting Information). Silica etching can be also achieved by simply adding a NaOH solution to the suspension containing Pt@SiO$_2$ and subsequently stirring for several minutes, which demonstrates the possibility of a facile and sequential process. To test the feasibility of large-scale synthesis, the growth of Pt-on-Au nanodendrites was carried out in a highly concentrated 40 mL of a mixture suspension containing Na_2PtCl_4 (3.6 g, 90 mg mL^{-1}), L-ascorbic acid (2.6 g, 66 mg mL^{-1}), and Au@*h*-SiO$_2$ nanospheres (1.8 g,

45 mg mL^{-1}), with subsequent treatment with a dilute NaOH solution (see Figure S4 in the Supporting Information). This single-step reaction produced as much as 1.5 g of uniform Lf-PtND in a ligand-free state with an overall yield of 81 % based on the initial amount of Pt used (Figure 3 b,c). Although the as-synthesized Lf-PtNDs lost their colloidal stability within 1 h when dispersed in water, they could be redispersed easily by simple vortexing and sonication.

To evaluate the effectiveness of the Lf-PtND as a catalyst for cathodes in PEMFCs, the activity of Lf-PtND toward ORR was compared with that of commercial Pt black catalysts (Alfa Aesar, HiSPEC fuel-cell grade) and spherical Pt/Au alloy nanocrystals prepared by reductive annealing of Pt@SiO_2 at 400 °C and subsequent etching of the silica shell (see Figure S5 in the Supporting Information). Figure 4 shows

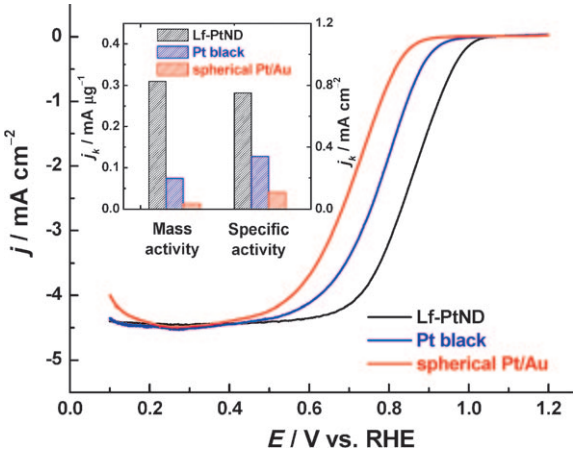

Figure 4. ORR polarization curves for Lf-PtND (black), Pt black (blue), and spherical Pt/Au (red) obtained in a 0.1 M $HClO_4$ solution saturated with O_2 with a scan rate of 10 mV s^{-1} and a rotation rate of 1600 rpm. Inset shows the mass and specific activities for three catalysts at 0.85 V. RHE = reversible hydrogen electrode.

the ORR polarization curves obtained in O_2-staurated 0.1 M $HClO_4$ solutions on a glassy carbon rotating disk electrode (RDE) loaded with 15.3 μg cm^{-2} of each catalyst. The polarization curve of Lf-PtND exhibited a positive shift of approximately 140 mV in both half-wave and onset potentials compared to the spherical Pt/Au alloy nanocrystals, which results in significantly improved electrocatalytic performance of Lf-PtND compared to spherical nanocrystals (Figure 4, inset). The mass and specific activities of Lf-PtND toward ORR at 0.85 V were much higher than those of the spherical Pt/Au alloy nanocrystals, which clearly demonstrates the effectiveness of the dendritic morphology of Pt nanocrystals as ORR catalysts over spherical ones. The markedly enhanced electrocatalytic activity of Lf-PtND was attributed to the presence of a large number of edges and corner atoms, as well as to the high catalytically effective surface area.[6a,8b] The electrochemical surface area (ECSA, see Figure S6 and Table S1 in the Supporting Information) of Lf-PtND (41.4 m^2 g^{-1}) was 3.5 times higher than that of the spherical Pt/Au alloy nanocrystals based on the mass of Pt catalyst. Moreover, Lf-PtND was found to exhibit approximately four times higher mass activity than the commercial Pt black catalysts, which is a similar enhancement to that reported for Pt-on-Pd dendrites versus Pt black catalysts.[8b] The higher mass activity showed that the use of Lf-PtND as an ORR catalyst is promising from an economic point of view. The examination of Lf-PtND catalysts as cathode materials in actual PEM fuel-cell environments, including the durability test, is under investigation. The N_2 adsorption–desorption isotherm of the Lf-PtND powder revealed a smaller surface area (25 m^2 g^{-1}) than the ECAS, which is most likely due to the sintering of the ligand-free surface during the outgassing procedure at 300 °C prior to the BET measurement.

In addition to the synthesis of Lf-PtND, the current synthetic procedure is widely applicable to the fabrication of well-dispersed colloidal nanocrystals and various hybrid nanocrystals, as outlined in Scheme 1. For example, capping the surface of Pt-on-Au nanodendrites with thiol ligands by adding either an aqueous solution of 3-mercaptopropionic acid or a hexane solution of 1-hexadecanethiol to an aqueous NaOH suspension of Pt@SiO_2 produced well-dispersed colloidal solutions of Pt-on-Au nanodendrites in either water or hexane, respectively.[14] The purified suspension of thiol-capped Pt-on-Au nanodendrites exhibited good colloidal stability with no aggregation detected after leaving the suspension to stand for more than one month at room temperature (see Figure S7 in the Supporting Information). The reduction of $HAuCl_4$, $AgNO_3$, or Na_2PdCl_4 in the suspension containing Pt@*h*-SiO_2 nanospheres with half-grown Pt-on-Au nanodendrite leads to the subsequent growth of gold, silver, and palladium on the nanodendrites, respectively, creating hybrid nanocrystals inside the cavity. Thermal annealing of the hybrid nanocrystals coated with a silica shell induced the transformation of their morphology and crystallinity in the solid state while preserving their nanocrystalline nature, leading to nanocrystals with altered heterojunction structures (Figure 5).

In summary, a novel method for synthesizing platinum-based nanocrystals with a uniform dendritic structure was developed based on seed-mediated growth inside hollow silica nanospheres. The newly developed procedure produced Pt-on-Au nanodendrites in a ligand-free form on a gram scale from a highly concentrated reaction suspension. The higher effectiveness of the Pt-on-Au nanodendrites as an electrocatalytic material for facilitating the oxygen reduction reaction was demonstrated compared to that of commercial Pt black catalysts. The procedure described herein can be developed as a generalized method to synthesize a wide range of hybrid nanocrystals and colloidal nanoparticles.

Experimental Section

Gram-scale synthesis of Lf-PtND: Au@*h*-SiO_2 nanospheres (1.8 g) were prepared by selectively etching Fe_3O_4 from silica nanospheres encapsulating a Fe_3O_4/Au hybrid nanocrystal (3.6 g) using the reported procedure including treatment with $NaBH_4$ in an aqueous suspension.[11] For the growth of Pt-on-Au nanodendrites, Au@*h*-SiO_2 nanospheres (1.8 g) and L-ascorbic acid (2.6 g) were mixed in an aqueous suspension (21 mL). A Na_2PtCl_4 solution (19 mL, 0.5 M) was then added dropwise to the mixed suspension over 1 min and stirred at room temperature for 3 h. The reaction suspension gradually

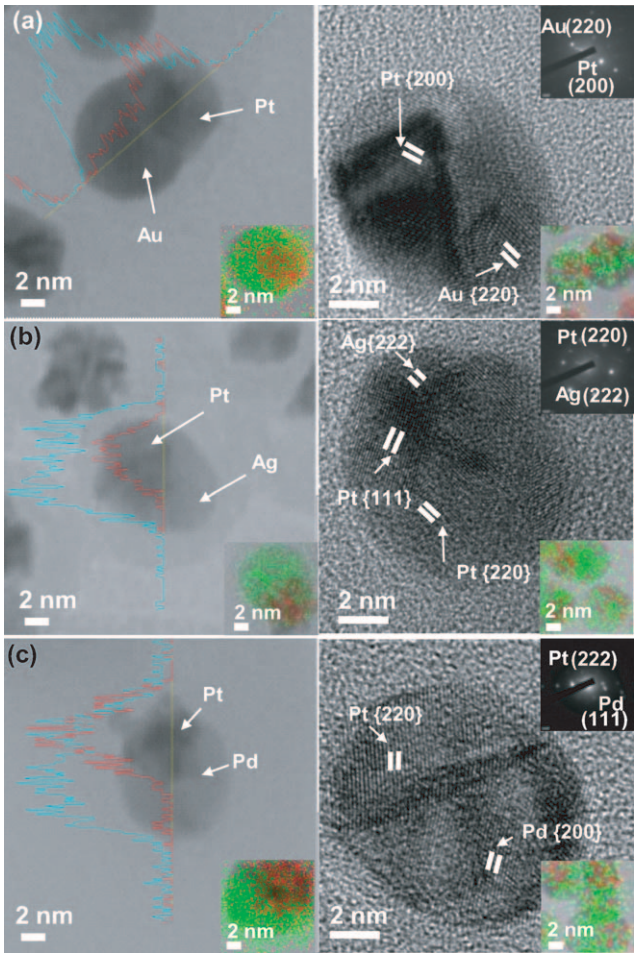

Figure 5. STEM images (left) of the hybrid nanocrystals a) Pt/Au@SiO_2, b) Pt/Ag@SiO_2, and c) Pt/Pd@SiO_2 with EDX elementary maps (insets) and line profiles showing the distribution of Pt (red dots and red lines) and other metal species (green dots and blue lines). TEM images (right) show the hybrid nanocrystals after annealing in a reductive environment at 400 °C for 2 h. Insets show EDX elementary maps and SAED patterns.

darkened, and an opaque black suspension was generated. The resulting solid Pt@SiO_2 was collected by centrifugation and washed with water by three cycles of dispersion in water and centrifugation. The purified solid Pt@SiO_2 was redispersed in aqueous NaOH (300 mL, 2.0 M) and stirred at room temperature, generating a turbid suspension within 3 h. The resulting solids were collected by centrifugation of the suspension and purified by washing with water. The resulting solids were dried in vacuo to give Lf-PtND as a black powder (1.5 g).

Received: September 15, 2010
Revised: October 13, 2010
Published online: December 14, 2010

Keywords: electrochemistry · heterogeneous catalysis · nanostructures · oxygen reduction · platinum

[1] A. Chen, P. Holt-Hindle, *Chem. Rev.* **2010**, *110*, 3767.
[2] a) F. A. de Bruijn, V. A. T. Dam, G. J. M. Janssen, *Fuel Cells* **2008**, *8*, 3; b) H. A. Gasteiger, S. S. Kocha, B. Sompalli, F. T. Wagner, *Appl. Catal. B* **2005**, *56*, 9.
[3] a) Z. Peng, H. Yang, *Nano Today* **2009**, *4*, 143; b) J. Y. Chen, B. Lim, E. P. Lee, Y. N. Xia, *Nano Today* **2009**, *4*, 81; c) M. Subhramannia, V. K. Pillai, *J. Mater. Chem.* **2008**, *18*, 5858.
[4] a) C. Wang, H. Daimon, T. Onodera, T. Koda, S. Sun, *Angew. Chem.* **2008**, *120*, 3644; *Angew. Chem. Int. Ed.* **2008**, *47*, 3588; b) N. Tian, Z.-Y. Zhou, S.-G. Sun, *J. Phys. Chem. C* **2008**, *112*, 19801; c) C. Wang, H. Daimon, Y. Lee, J. Kim, S. Sun, *J. Am. Chem. Soc.* **2007**, *129*, 6974; d) N. Tian, Z. Y. Zhou, S. G. Sun, Y. Ding, Z. L. Wang, *Science* **2007**, *316*, 732.
[5] a) J. Kim, Y. Lee, S. Sun, *J. Am. Chem. Soc.* **2010**, *132*, 4996; b) Z. Peng, H. Yang, *J. Am. Chem. Soc.* **2009**, *131*, 7542; c) J. Zhang, K. Sasaki, E. Sutter, R. R. Adzic, *Science* **2007**, *315*, 220; d) V. R. Stamenkovic, B. Fowler, B. S. Mun, G. F. Wang, P. N. Ross, C. A. Lucas, N. M. Markovic, *Science* **2007**, *315*, 493.
[6] a) B. Lim, X. M. Lu, M. J. Jiang, P. H. C. Camargo, E. C. Cho, E. P. Lee, Y. N. Xia, *Nano Lett.* **2008**, *8*, 4043; b) L. Wang, S. J. Guo, J. F. Zhai, S. J. Dong, *J. Phys. Chem. C* **2008**, *112*, 13372; c) Y. J. Song, W. A. Steen, D. Peña, Y. B. Jiang, C. J. Medforth, Q. Huo, J. L. Pincus, Y. Qiu, D. Y. Sasaki, J. E. Miller, J. A. Shelnutt, *Chem. Mater.* **2006**, *18*, 2335; d) M. H. Ullah, W. S. Chung, I. Kim, C. S. Ha, *Small* **2006**, *2*, 870.
[7] a) Z. H. Lin, M. H. Lin, H. T. Chang, *Chem. Eur. J.* **2009**, *15*, 4656; b) M. A. Mahmoud, C. E. Tabor, M. A. El-Sayed, Y. Ding, Z. L. Wang, *J. Am. Chem. Soc.* **2008**, *130*, 4590; c) X. Teng, X. Liang, S. Maksimuk, H. Yang, *Small* **2006**, *2*, 249; d) Y. Song, Y. Yang, C. J. Medforth, E. Pereira, A. K. Singh, H. Xu, Y. Jiang, C. J. Brinker, F. van Swol, J. A. Shelnutt, *J. Am. Chem. Soc.* **2004**, *126*, 635.
[8] a) S. Guo, S. Dong, E. Wang, *ACS Nano* **2010**, *4*, 547; b) B. Lim, M. Jiang, P. H. C. Camargo, E. C. Cho, J. Tao, X. Lu, Y. Zhu, Y. Xia, *Science* **2009**, *324*, 1302.
[9] For a recent review on the surfactant-assisted synthesis of nanostructures, see: Y. Yamauchi, K. Kuroda, *Chem. Asian J.* **2008**, *3*, 664.
[10] a) L. Wang, H. Wang, Y. Nemoto, Y. Yamauchi, *Chem. Mater.* **2010**, *22*, 2835; b) L. Wang, Y. Yamauchi, *J. Am. Chem. Soc.* **2009**, *131*, 9152.
[11] K. M. Yeo, J. Shin, I. S. Lee, *Chem. Commun.* **2010**, *46*, 64.
[12] a) H. Ataee-Esfahani, L. Wang, Y. Yamauchi, *Chem. Commun.* **2010**, *46*, 3684; b) S. Y. Wang, N. Kristian, S. P. Jiang, X. Wang, *Nanotechnology* **2009**, *20*, 025605; c) S. G. Zhou, K. McIlwrath, G. Jackson, B. Eichhorn, *J. Am. Chem. Soc.* **2006**, *128*, 1780.
[13] L. Colombi Ciacchi, W. Pompe, A. D. Vita, *J. Phys. Chem. B* **2003**, *107*, 1755.
[14] J. Kim, C. Rong, J. P. Liu, S. Sun, *Adv. Mater.* **2009**, *21*, 906.